

## Solid-State Structure and Solution Behavior of Eight-Coordinate Sm(III) Poly(pyrazolyl)-borate Compounds

Irene Lopes,<sup>†</sup> Anna C. Hillier,<sup>‡</sup> Sung Ying Liu,<sup>‡</sup> Ângela Domingos,<sup>†</sup> José Ascenso,<sup>§</sup> Adelino Galvão,<sup>§</sup> Andrea Sella,<sup>\*,‡</sup> and Noémia Marques<sup>\*,†,||</sup>

Departamento de Química, ITN, Estrada Nacional 10, P-2686, Sacavém Codex, Portugal, Department of Chemistry, Christopher Ingold Laboratories, University College of London, 20 Gordon Street, London, WC1H 0AJ, U.K., and Departamento de Engenharia Química, Instituto Superior Técnico, P-1096 Lisboa Codex, Portugal

Received September 19, 2000

[Sm(Tp<sup>Me</sup>)<sub>2</sub>(κ<sup>2</sup>-S<sub>2</sub>CNR<sub>2</sub>)] compounds (R = Et (**1**), Me (**2**); Tp<sup>Me</sup> = HB(3,5-Me<sub>2</sub>pz)<sub>3</sub>) have been isolated from reaction of (R<sub>2</sub>NC(S)S)<sub>2</sub> with 2 equiv of [Sm(Tp<sup>Me</sup>)<sub>2</sub>]. Reductive cleavage of 2,2'-dipyridyl disulfide or 2,2'-dipyridyl diselenide by [Sm(Tp<sup>Me</sup>)<sub>2</sub>] afforded good yields of [Sm(Tp<sup>Me</sup>)<sub>2</sub>(κ<sup>2</sup>-Y)] compounds (Y = 2-SC<sub>5</sub>H<sub>4</sub>N (**3**), 2-SeC<sub>5</sub>H<sub>4</sub>N (**4**)). **4** is the first selenopyridine complex of an f-block element. Sm(Tp<sup>Me</sup>)<sub>2</sub>(2-OC<sub>5</sub>H<sub>4</sub>N) (**5**) has been synthesized by salt metathesis of [Sm(Tp<sup>Me</sup>)<sub>2</sub>Cl] with the sodium salt of the 2-hydroxypyridine. The solid-state structures of **1**, **3**, **4**, and **5** were determined by single-crystal X-ray diffraction analysis and revealed that the compounds are all eight-coordinate with dodecahedral geometry. The samarium atoms are bound in tridentate fashion to two pyrazolylborate ligands and in bidentate fashion by the third ligand. The solution behavior of the compounds was studied by <sup>1</sup>H NMR techniques. <sup>1</sup>H–<sup>1</sup>H exchange spectroscopy experiments give evidence for two distinct dynamic regimes occurring in solution.

### Introduction

Although the bis(pentamethylcyclopentadienyl) ligand system has been responsible for the major advances in organometallic chemistry of lanthanides for the past 2 decades,<sup>1</sup> the recognition that the ligand environment plays a dominant role in determining the reactivity of the compounds led to the development of new ligand sets as alternatives to cyclopentadienyl ligands.<sup>2</sup> The hydrotris(pyrazolyl)borate ligands (Tp<sup>R</sup>), which have found numerous applications in coordination chemistry throughout the periodic table,<sup>3</sup> are a class of ligands that are particularly suitable for stabilizing both lanthanide(II) and lanthanide(III) ions.<sup>3,4</sup> Recently, several complexes of the type [Sm(Tp<sup>Me</sup>)<sub>2</sub>X] (X = PhNNPh, O<sub>2</sub>, OCPH<sub>2</sub>, quinone, halide) have been prepared and structurally characterized.<sup>5</sup> The stability of these complexes was ascribed to the steric protection provided by the “Sm(Tp<sup>Me</sup>)<sub>2</sub>” moiety. Despite the steric congestion imparted to the coordination sphere by this ligand set, some of us have found that in the series [Ln(Tp<sup>Me</sup>)<sub>2</sub>(O<sub>3</sub>SCF<sub>3</sub>)(MeCN)<sub>2</sub>] (La–Nd) it was

possible to accommodate additional neutral ligands in the coordination sphere of the metal ion increasing its coordination number beyond 7.<sup>6</sup> The crystal structures of [La(Tp<sup>Me</sup>)<sub>2</sub>(O<sub>3</sub>-SCF<sub>3</sub>)(MeCN)]·MeCN and [Nd(Tp<sup>Me</sup>)<sub>2</sub>(MeCN)<sub>2</sub>][O<sub>3</sub>SCF<sub>3</sub>] have been determined, and it was shown that the coordination geometry around the metal in both complexes was dodecahedral, in contrast to the square antiprismatic geometry found in most of the complexes involving unsubstituted hydrotris(pyrazolyl)borate.<sup>4</sup> We intended to verify whether eight-coordinate complexes could also be achieved for the smaller Sm(III) ion. With this purpose in mind we chose potentially chelating ligands with different bites to test the limits of steric protection provided by the “Sm(Tp<sup>Me</sup>)<sub>2</sub>” fragment. Here we report the synthesis, the solid-state structure, and solution behavior of a series of samarium compounds of the type Sm(Tp<sup>Me</sup>)<sub>2</sub>L with L being a bidentate ligand (L = S<sub>2</sub>CNEt<sub>2</sub>, S<sub>2</sub>CNMe<sub>2</sub>, 2-SC<sub>5</sub>H<sub>4</sub>N, 2-SeC<sub>5</sub>H<sub>4</sub>N, 2-OC<sub>5</sub>H<sub>4</sub>N).

### Experimental Section

**General Procedures.** All operations were performed using standard Schlenk line and drybox techniques under an inert atmosphere of nitrogen. THF, toluene, and *n*-hexane were dried by standard methods and degassed prior to use. Deuterated solvents, benzene-*d*<sub>6</sub>, and toluene-*d*<sub>8</sub> were dried over Na or Na/K alloy and distilled. [Sm(Tp<sup>Me</sup>)<sub>2</sub>], [Sm-

<sup>†</sup> ITN.

<sup>‡</sup> University College of London.

<sup>§</sup> Instituto Superior Técnico.

<sup>||</sup> E-mail: nmarques@itn1.itn.pt. Fax: 351-1-9941455.

- (1) For recent reviews, see the following. (a) Edlmann, F. T. *Compr. Organomet. Chem. II* **1996**, *4*, 11–212. (b) Edlmann, F. T. In *Metalloenes: Synthesis, Reactivity, Applications*; Togni, A., Halterman, R. L., Eds.; Wiley-VCH: Weinheim, 1998; Vol. 1, p 55–104. (c) Schumann, H.; Meese-Marktscheffel, J. A.; Esser, L. *Chem. Rev.* **1995**, *865*–986. (d) Schaverien, C. J. *Adv. Organomet. Chem.* **1994**, *36*, 283–362.
- (2) Edlmann, F. T. *Angew. Chem., Int. Ed. Engl.* **1995**, *34*, 2466–2488.
- (3) (a) Trofimenko, S. In *Scorpionates: The Coordination Chemistry of Polypyrazolylborate Ligands*; Imperial College Press: River Edge, NJ, 1999. (b) Trofimenko, S. *Chem. Rev.* **1993**, *93*, 943–980. (c) Kitajima, N.; Tolman, W. B. *Prog. Inorg. Chem.* **1995**, *43*, 419–531. (d) Reger, D. L. *Coord. Chem. Rev.* **1996**, *147*, 571–595. (e) Etienne, M. *Coord. Chem. Rev.* **1997**, *156*, 201–236.
- (4) Santos, I.; Marques, N. *New J. Chem.* **1995**, *19*, 551–571.

- (5) (a) Takats, J.; Zhang, X. W.; Day, V. W.; Eberspacher, T. A. *Organometallics* **1993**, *12*, 4286–4288. (b) Zhang, X. W.; Lopponow, G. R.; McDonald, R.; Takats, J. *J. Am. Chem. Soc.* **1995**, *117*, 7828–7829. (c) Takats, J. *J. Alloys Compd.* **1997**, *249*, 52. (d) Lin, G. Y.; Lopes, I.; Zhang, X. W.; Domingos, A.; Marques, N.; Takats, J. Manuscript in preparation. (e) Hillier, A. C.; Zhang, X. W.; Maunder, G. H.; Liu, S. Y.; Eberspacher, T. A.; Metz, M. V.; McDonald, R.; Domingos, A.; Marques, N.; Day, V. W.; Sella, A.; Takats, J. Manuscript in preparation.
- (6) Clark, R. J. H.; Liu, S.-Y.; Maunder, G. H.; Sella, A.; Elsegood, M. R. *J. Chem. Soc., Dalton Trans.* **1997**, 2241–2247.

( $\text{Tp}^{\text{Me}_2}$ ) $_2\text{Cl}$ ],<sup>5a,5c</sup> and  $(\text{C}_5\text{H}_4\text{N})_2\text{Se}_2$ <sup>7</sup> were synthesized according to published methods.  $\text{KO}(\text{C}_5\text{H}_4\text{N})$  was prepared by reacting 1 equiv of KH with hydroxypyridine in THF. Dithiuram disulfides were purchased from Aldrich and used without further purification.  $(\text{C}_5\text{H}_4\text{N})_2\text{S}_2$  ("Aldrithiol") was also purchased from Aldrich and sublimed before use.  $^1\text{H}$  NMR spectra were recorded on Bruker AMX 400 (UCL) or on Varian VXR 300 (Sacavém) spectrometers and referenced internally using the residual solvent resonances relative to tetramethylsilane.  $^1\text{H}$  phase-sensitive exchange spectroscopy (EXSY) experiments were recorded with a Bruker Avance 500 spectrometer using standard Bruker software with a mixing time of 500 ms and recycle delays of 2 s. IR spectra were recorded on a Perkin-Elmer 2000 FT-IR spectrometer. Carbon, hydrogen, and nitrogen analyses were performed in-house using Perkin-Elmer automatic analyzers.

**Synthetic Procedures.** [ $\text{Sm}(\text{Tp}^{\text{Me}_2})_2(\text{S}_2\text{CNEt}_2)$ ], **1**. To a slurry of [ $\text{Sm}(\text{Tp}^{\text{Me}_2})_2$ ] (205 mg, 0.28 mmol) in toluene (10 cm<sup>3</sup>) at  $-78^\circ\text{C}$  was added a solution of tetraethylthiuram disulfide (38 mg, 0.14 mmol) in toluene (10 cm<sup>3</sup>). The mixture was stirred overnight, during which time it became pale-yellow. The solution was filtered and the toluene removed under reduced pressure. The pale-yellow solid was dissolved in Et<sub>2</sub>O and the volume reduced to ca. 5 mL. Slow cooling to  $-30^\circ\text{C}$  gave a pale-yellow solid. Yield: 143 mg (0.16 mmol), 59%. Anal. Calcd for  $\text{C}_{35}\text{H}_{54}\text{N}_{13}\text{B}_2\text{S}_2\text{Sm}$ : C, 47.07; H, 6.09; N, 20.39. Found: C, 46.35; H, 6.31; N, 19.59. IR (KBr, cm<sup>-1</sup>): 2557, 2525 (BH); 1476 (CN); 1008 (CS).  $^1\text{H}$  NMR (CDCl<sub>3</sub>, 253 K):  $-5.37$  (s, 6H, 3-Me), 0.53 (s, 6H, 3-Me), 1.25 (t, CH<sub>2</sub>-CH<sub>3</sub>), 2.44 (s, 6H, 5-Me), 2.69 (s, 6H, 5-Me), 3.10 (s, 6H, 5-Me), 3.29 (s, 6H, 3-Me), 4.10 (br, 4H, CH<sub>2</sub>-CH<sub>3</sub>), 5.09 (s, 2H, 4-CH-pz), 5.55 (s, 2H, 4-CH-pz), 6.27 (s, 2H, 4-CH-pz).

[ $\text{Sm}(\text{Tp}^{\text{Me}_2})_2(\text{S}_2\text{CNMe}_2)$ ], **2**. **2** was prepared analogously to **1** using dimethylthiuram disulfide but was isolated by slow cooling of a concentrated toluene solution to give a pale-yellow solid. Elemental microanalysis calculated for  $\text{C}_{33}\text{H}_{50}\text{N}_{13}\text{B}_2\text{S}_2\text{Sm}\cdot 0.25\text{C}_7\text{H}_8$ : C, 47.0; H, 5.90; N 20.51. Found: C, 46.44; H, 5.81; N, 19.42. IR (KBr, cm<sup>-1</sup>): 2557, 2525 (BH); 1476 (CN); 1008 (CS).  $^1\text{H}$  NMR (CDCl<sub>3</sub>, 253 K):  $-4.82$  (s, 6H, 3-Me), 0.65 (s, 6H, 3-Me), 2.39 (s, 6H, 5-Me), 2.67 (s, 6H, 5-Me), 3.09 (s, 6H, 5-Me), 3.37 (s, 6H, 3-Me), 4.63 (s, 6H, NMe), 5.09 (s, 2H, 4-CH-pz), 5.61 (s, 2H, 4-CH-pz), 6.31 (s, 2H, 4-CH-pz).

[ $\text{Sm}(\text{Tp}^{\text{Me}_2})_2(\text{SC}_5\text{H}_4\text{N})$ ], **3**. To a slurry of [ $\text{Sm}(\text{Tp}^{\text{Me}_2})_2$ ] (230 mg, 0.31 mmol) in toluene (20 cm<sup>3</sup>) was added  $(\text{C}_5\text{H}_4\text{N})_2\text{S}_2$  (34 mg, 0.15 mmol) in the same solvent (10 cm<sup>3</sup>). Reaction occurred instantaneously to give a yellow solution. Stirring was continued for 2 h. Removal of solvent under reduced pressure yielded a light-yellow microcrystalline solid. Yield: 70% (190 mg, 0.22 mmol). Crystals obtained from toluene/hexane mixtures were not adequate for X-ray diffraction analysis, but recrystallization from a benzene solution layered with hexane gave crystals of good quality. Anal. Calcd for  $\text{C}_{33}\text{H}_{48}\text{N}_{13}\text{B}_2\text{SSm}$ : C, 49.18; H, 5.62; N, 21.31. Found: C, 50.01; H, 5.83; N, 19.96. IR (Nujol, cm<sup>-1</sup>): 2551, 2503 (BH).  $^1\text{H}$  NMR (C<sub>6</sub>D<sub>6</sub>, 293 K,  $\delta$  ppm):  $-2.48$  (s, 3H, 3-Me),  $-2.31$  (s, 3H, 3-Me), 0.78 (s, 3H, 3-Me), 1.61 (s, 3H, 3-Me), 1.73 (s, 3H, 5-Me), 2.00 (s, 3H, 5-Me), 2.08 (s, 3H, 5-Me), 2.15 (s, 3H, 5-Me), 2.33 (s, 3H, 5-Me), 2.60 (s, 3H, 5-Me), 3.87 (s, 3H, 3-Me), 4.28 (s, 3H, 3-Me), 4.85 (1H, 4-CH-pz), 4.98 (1H, 4-CH-pz), 5.39 (1H, 4-CH-pz), 5.42 (1H, 4-CH-pz), 6.12 (1H, 4-CH-pz), 6.28 (1H, 4-CH-pz), 6.72 (m, 1H, H(5)), 7.58 (d, 1H, H(6)), 7.71 (m, 1H, H(4)), 9.18 (d, 1H, H(3)).

[ $\text{Sm}(\text{Tp}^{\text{Me}_2})_2(\text{SeC}_5\text{H}_4\text{N})$ ], **4**. In a similar fashion,  $(\text{C}_5\text{H}_4\text{N})_2\text{Se}_2$  (40 mg, 0.128 mmol) in toluene solution was added to a slurry of [ $\text{Sm}(\text{Tp}^{\text{Me}_2})_2$ ] (190 mg, 0.256 mmol) in toluene. The yellow compound was isolated as described for **3**. Yield: 60% (138 mg, 0.164 mmol). Crystals suitable for X-ray diffraction analysis were obtained from a toluene/hexane mixture. Anal. Calcd for  $\text{C}_{33}\text{H}_{48}\text{N}_{13}\text{B}_2\text{SeSm}$ : C, 46.62; H, 5.33; N, 20.20. Found: C, 46.30; H, 5.50; N, 18.77. IR (Nujol, cm<sup>-1</sup>): 2530, 2510 (BH).  $^1\text{H}$  NMR (C<sub>6</sub>D<sub>6</sub>, 293 K,  $\delta$  ppm):  $-2.07$  (s, 3H, 3-Me),  $-1.90$  (s, 3H, 3-Me), 0.90 (s, 3H, 3-Me), 1.67 (s, 3H, 3-Me), 1.71 (s, 3H, 5-Me), 1.96 (s, 3H, 5-Me), 2.04 (s, 3H, 5-Me), 2.10 (s, 3H, 5-Me), 2.28 (s, 3H, 5-Me), 2.53 (s, 3H, 5-Me), 3.91 (s, 3H, 3-Me), 4.03 (s, 3H, 3-Me), 4.84 (s, 1H, 4-CH-pz), 5.05 (s, 1H, 4-CH-pz), 5.40 (s, 1H, 4-CH-pz), 5.44 (s, 1H, 4-CH-pz), 6.13 (s, 1H, 4-CH-pz), 6.26 (s, 1H, 4-CH-pz), 6.72 (t, 1H, H(5)), 7.48 (t, 1H, H(4)) 7.59 (d, 1H, H(6)), 9.28 (d, 1H, H(3)).

[ $\text{Sm}(\text{Tp}^{\text{Me}_2})_2(\text{OC}_5\text{H}_4\text{N})$ ], **5**. To a solution of [ $\text{Sm}(\text{Tp}^{\text{Me}_2})_2\text{Cl}$ ] (360 mg, 0.46 mmol) in THF (20 cm<sup>3</sup>) was slowly added a solution of  $\text{KOC}_5\text{H}_4\text{N}$  (61 mg, 0.46 mmol) in the same solvent (15 cm<sup>3</sup>). After the solution was stirred overnight, the precipitate of KCl was discharged and the solvent was removed from the resulting solution under reduced pressure. Colorless crystals were obtained from a THF/hexane mixture. Analytically pure **5** was obtained by decanting off the mother liquor and drying under vacuum. Yield: 70% (270 mg, 0.23 mmol). Crystals suitable for X-ray diffraction analysis were obtained from a toluene/hexane mixture. Anal. Calcd for  $\text{C}_{35}\text{H}_{48}\text{N}_{13}\text{B}_2\text{OSm}$ : C, 50.12; H, 5.77; N, 21.71. Found: C, 50.71; H, 5.75; N, 22.42. IR (Nujol, cm<sup>-1</sup>): 2540, 2500 (BH).  $^1\text{H}$  NMR (CD<sub>2</sub>Cl<sub>2</sub>, 293 K,  $\delta$  ppm): 0.06 (s, 18H, vbr, 3-Me), 2.54 (s, 18H, 5-Me), 4.8 (vbr, 2H, B-H), 5.54 (s, 6H, 4-CH-pz), 6.87 (t, 1H, H(5)), 7.28 (d, 1H, H(6)), 8.63 (t, 1H, H(4)), 9.36 (d, 1H, H(3)).  $^1\text{H}$  NMR (CD<sub>2</sub>Cl<sub>2</sub>, 193 K,  $\delta$  ppm):  $-6.66$  (s, 3H, 3-Me),  $-6.61$  (s, 3H, 3-Me),  $-1.02$  (s, 3H, 3-Me), 0.87 (s, 3H, 3-Me), 2.41 (s, 3H, 5-Me), 2.43 (s, 3H, 5-Me), 2.75 (s, 3H, 5-Me), 2.86 (s, 3H, 5-Me), 2.93 (s, 3H, 5-Me), 2.99 (s, 3H, 5-Me), 3.08 (s, 3H, 3-Me), 4.03 (s, 3H, 3-Me), 5.11 (s, 1H, 4-CH-pz), 5.15 (s, 1H, 4-CH-pz), 5.39 (s, 1H, 4-CH-pz), 5.51 (s, 1H, 4-CH-pz), 6.48 (s, 1H, 4-CH-pz), 6.82 (s, 1H, 4-CH-pz), 7.25 (t, 1H, H(5)), 8.07 (d, 1H, H(6)), 8.76 (t, 1H, H(4)), 9.27 (d, 1H, H(3)).

[ $\text{Nd}(\text{Tp}^{\text{Me}_2})_2(\text{OC}_5\text{H}_4\text{N})$ ], **6**. To a solution of [ $\text{Nd}(\text{Tp}^{\text{Me}_2})_2\text{Cl}$ ] (145 mg, 0.19 mmol) in THF (15 cm<sup>3</sup>) was slowly added a solution of  $\text{KOC}_5\text{H}_4\text{N}$  (25 mg, 0.19 mmol) in the same solvent (10 cm<sup>3</sup>). **6** was isolated by the procedure described above for **5**. Yield: 64% (100 mg, 0.120 mmol). Anal. Calcd for  $\text{C}_{35}\text{H}_{48}\text{N}_{13}\text{B}_2\text{ONd}$ : C, 50.48; H, 5.81; N, 21.87. Found: C, 47.81; H, 5.92; N, 19.21. IR (Nujol, cm<sup>-1</sup>): 2540 (sh), 2502 (BH).  $^1\text{H}$  NMR (CD<sub>2</sub>Cl<sub>2</sub>, 293 K,  $\delta$  ppm): 1.43 (vbr, 18H, 5-Me), 12.40 (t, 1H, Opy), 12.66 (d, 1H, Opy), 16.06 (t, 1H, Opy), 28.50 (d, 1H, Opy). (The resonances due to 3-Me and 4-CH-pz were collapsed into the baseline.)  $^1\text{H}$  NMR (CD<sub>2</sub>Cl<sub>2</sub>, 196 K,  $\delta$  ppm):  $-54.09$  (s, 3H, Me-pz),  $-53.41$  (s, 3H, Me-pz),  $-19.86$  (s, 3H, Me-pz),  $-6.32$  (s, 3H, Me-pz),  $-5.28$  (s, 3H, Me-pz),  $-4.55$  (s, 1H, 4-CH-pz),  $-2.73$  (s, 1H, 4-CH-pz),  $-0.22$  (s, 3H, Me-pz), 1.37 (s, 3H, Me-pz), 1.74 (s, 3H, Me-pz), 6.20 (s, 3H, Me-pz), 6.38 (s, 3H, Me-pz), 7.26 (s, 1H, 4-CH-pz), 11.59 (s, 1H, 4-CH-pz), 14.87 (1H, Opy), 16.13 (s, 3H, Me-pz), 17.37 (1H, Opy), 19.28 (s, 1H, 4-CH-pz), 21.25 (s, 1H, 4-CH-pz), 24.00 (1H, Opy), 51.48 (1H, Opy), 59.02 (s, 3H, Me-pz).

**X-ray Crystallographic Analysis.** A pale-yellow crystal of **1** was grown by slow cooling of a diethyl ether solution. Crystals of **3** (pale-yellow) were grown by slow diffusion of *n*-hexane into a benzene solution, and crystals of **4** and **5** (yellow and colorless, respectively) were grown from toluene/hexane mixtures. The crystals were mounted in thin-walled glass capillaries in a nitrogen-filled glovebox. Data in the range  $1.5^\circ < \theta < 25^\circ$  were collected at room temperature (except for **1** and **3**, which were collected at 150 and 278 K, respectively) on a Nonius Kappa CCD area detector diffractometer equipped with a rotating anode FR591 generator for **1**, and on an Enraf-Nonius CAD4-diffractometer for all the others, using graphite-monochromated Mo K $\alpha$  radiation. For **1** images of  $2^\circ$  thickness and 10 s exposure were taken in a  $360^\circ \phi$  scan, followed by five shorter  $\omega$  scans, with a detector to crystal distance of 30 mm ( $\theta$  offsets between  $3.3^\circ$  and  $9.95^\circ$ ) and processed by Denzo<sup>8</sup> to give 99.4% coverage of the unique data set. Data were corrected for absorption using DIFABS.<sup>9</sup> For **3**–**5** the  $\omega$ – $2\theta$  scan technique was used, and the data were corrected<sup>10</sup> for Lorentz and polarization effects, for linear decay, and empirically for absorption by  $\Psi$  scans. Table 1 summarizes the crystallographic data. The structures were solved by Patterson methods<sup>11</sup> and developed by alternating cycles of full-matrix least-squares refinement on  $F^2$  and difference Fourier techniques, using SHELXL-93.<sup>12</sup> For **3** there are three molecules of benzene present per formula unit. All the non-hydrogen

(7) Kienitz, C. O.; Thöne, C.; Jones, P. G. *Inorg. Chem.* **1996**, *35*, 3990–3997.

(8) Otwinowski, Z.; Minor, W. In *Macromolecular Crystallography, Part A*, Carter, C. W., Jr., Sweet, R. M., Eds.; Methods in Enzymology 276; Academic Press: San Diego, 1997.

(9) Walker, N.; Stuart, D. *Acta Crystallogr.* **1983**, *A39*, 158–166.

(10) Fair, C. K. *Molen*; Enraf-Nonius: Delft, The Netherlands, 1990.

(11) Sheldrick, G. M. *SHELXS-86: Program for Solution of Crystal Structure*; University of Göttingen: Göttingen, Germany, 1986.

**Table 1.** Crystallographic Data for Complexes **1**, **3**·3C<sub>6</sub>H<sub>6</sub>, and **5**

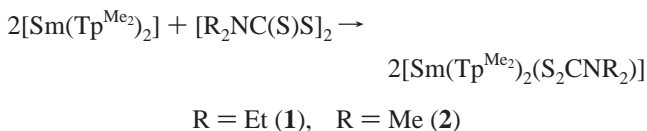
	<b>1</b>	<b>3</b> ·3C <sub>6</sub> H <sub>6</sub>	<b>5</b>
formula	C <sub>35</sub> H <sub>54</sub> B <sub>2</sub> N <sub>13</sub> S <sub>2</sub> Sm	C <sub>35</sub> H <sub>48</sub> B <sub>2</sub> N <sub>13</sub> SSm· 3C <sub>6</sub> H <sub>6</sub>	C <sub>35</sub> H <sub>48</sub> B <sub>2</sub> N <sub>13</sub> OSm
fw	893.00	1089.22	838.83
cryst syst	triclinic	triclinic	triclinic
space group	<i>P</i> 1	<i>P</i> 1	<i>P</i> 1
<i>a</i> , Å	11.459(2)	10.835(3)	10.881(4)
<i>b</i> , Å	12.787(3)	15.026(4)	10.927(3)
<i>c</i> , Å	15.062(3)	16.873(4)	19.737(4)
α, deg	84.19(3)	82.65(2)	76.63(1)
β, deg	82.14(3)	89.32(2)	75.98(1)
γ, deg	71.92(3)	86.61(2)	59.97(1)
<i>V</i> , Å <sup>3</sup>	2074.2(7)	2719.7(12)	1954.2(1)
<i>Z</i>	2	2	2
μ, mm <sup>-1</sup>	1.559	1.166	1.549
ρ <sub>calc</sub> , g cm <sup>-3</sup>	1.430	1.330	1.426
R1 <sup>a</sup>	0.0451	0.0950	0.0350
wR2 <sup>b</sup>	0.1181	0.1711	0.0728

<sup>a</sup> R1 =  $\sum |F_o| - |F_c| / \sum |F_o|$ . <sup>b</sup> wR2 =  $[\sum (w(F_o^2 - F_c^2)^2) / \sum (w(F_o^2)^2)]^{1/2}$ ;  $w = 1/[\sigma^2(F_o^2) + (aP)^2 + bP]$ , where  $P = (F_o^2 + 2F_c^2)/3$ . The values were calculated for data with  $I > 2\sigma(I)$ .

atoms were refined with anisotropic thermal motion parameters, and hydrogen atoms were placed in calculated positions (except those of the solvent molecules in **3**). The crystal structure of **4** was also determined on the basis of a twinned crystal. The molecular structure, however, was found to be disordered between two different conformations related by a mirror plane defined by the boron and the samarium atoms. This plane, coincident with a crystallographic mirror plane, emulates a *C*<sub>2</sub>/*m* space group from the twinned *C*<sub>2</sub> crystals of each conformer. Because of the poor quality of refinement resulting from the twinning, the Supporting Information will not be deposited but the relevant geometrical parameters will be given.<sup>13</sup>

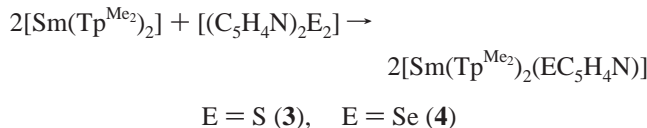
## Results and Discussion

**Synthesis and Characterization of Complexes [Sm(Tp<sup>Me</sup><sub>2</sub>)<sub>2</sub>L] (L = S<sub>2</sub>CNET<sub>2</sub>, S<sub>2</sub>CNMe<sub>2</sub>, SC<sub>5</sub>H<sub>4</sub>N, SeC<sub>5</sub>H<sub>4</sub>N, OC<sub>5</sub>H<sub>4</sub>N).** The reducing properties of [Sm(Tp<sup>Me</sup><sub>2</sub>)<sub>2</sub>] have been used to prepare the dithiocarbamate derivatives [Sm(Tp<sup>Me</sup><sub>2</sub>)<sub>2</sub>(S<sub>2</sub>-CNR<sub>2</sub>)] (R = Et (**1**), Me (**2**)). Addition of {R<sub>2</sub>NC(S)S}<sub>2</sub> to [Sm(Tp<sup>Me</sup><sub>2</sub>)<sub>2</sub>] in toluene resulted in the gradual disappearance of the purple color to give a clear solution on stirring overnight. Filtration and recrystallization from diethyl ether afforded the expected dithiocarbamate compounds, [Sm(Tp<sup>Me</sup><sub>2</sub>)<sub>2</sub>(S<sub>2</sub>CNET<sub>2</sub>)] (**1**) and [Sm(Tp<sup>Me</sup><sub>2</sub>)<sub>2</sub>(S<sub>2</sub>CNMe<sub>2</sub>)] (**2**), as pale-yellow crystalline materials in reasonable yield:



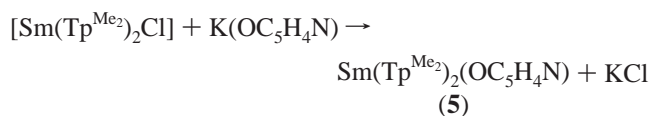
The reducing synthetic strategy was extended to the reaction with E<sub>2</sub>R<sub>2</sub> reagents.<sup>14</sup> Addition of dipyrindyl disulfide or dipyrindyl diselenide to a slurry of [Sm(Tp<sup>Me</sup><sub>2</sub>)<sub>2</sub>] in THF or toluene resulted

in the dissolution of the purple starting material to give yellow solutions, which after simple workup yielded the yellow monochalcogenide compounds [Sm(Tp<sup>Me</sup><sub>2</sub>)<sub>2</sub>(SC<sub>5</sub>H<sub>4</sub>N)] (**3**) and [Sm(Tp<sup>Me</sup><sub>2</sub>)<sub>2</sub>(SeC<sub>5</sub>H<sub>4</sub>N)] (**4**) in ca.60% yield:



Although thiopyridine complexes of the lanthanides are well-precedented we note that **4** is, to our knowledge the first selenopyridine complex of an f element. The first s-, p-, and d-block element complexes were first isolated in the mid-1990s.<sup>15</sup>

Metathesis of [Sm(Tp<sup>Me</sup><sub>2</sub>)<sub>2</sub>Cl] with the potassium salt of the hydroxypyridine in THF yielded [Sm(Tp<sup>Me</sup><sub>2</sub>)<sub>2</sub>(OC<sub>5</sub>H<sub>4</sub>N)] (**5**) in straightforward fashion:



The compounds were soluble in common aromatic and ethereal solvents. It was difficult, however, to obtain analytically pure solids, although the NMR spectra (vide infra) showed no evidence for significant impurities. Similar problems have been encountered before in these systems. The infrared spectra were found to exhibit ν(B–H) stretching vibrations as a doublet in the range 2500–2550 cm<sup>-1</sup>, consistent with tridentate Tp<sup>Me</sup><sub>2</sub> ligands.<sup>16</sup> In the spectra of **1** and **2** a strong band around 1476 cm<sup>-1</sup> indicated the presence of a bound dithiocarbamate ligand.

In solution the <sup>1</sup>H NMR spectra of **1** and **2** at room temperature exhibited resonances associated with the dithiocarbamate protons (a triplet and a quartet for **1** and a singlet for **2**) together with six broad singlets assigned to the Tp<sup>Me</sup><sub>2</sub> methyl protons and three for the pyrazolyl ring protons. Cooling the samples resulted in sharpening of the nine pyrazolyl peaks. The room temperature <sup>1</sup>H NMR spectra of **3** and **4** showed the expected integration and peak multiplicities for the chalcogenolate protons. In addition, however, the spectra featured 12 singlets due to the methyl groups and 6 due to the H(4) protons. When complexes **1**–**4** in toluene-*d*<sub>8</sub> were warmed, the peaks associated with the pyrazolylborate ligands began to broaden but a limiting spectrum could not be reached. Thus, the observed spectra are consistent with C<sub>2</sub>-symmetric structures for **1** and **2** and C<sub>1</sub>-symmetric structures for **3** and **4**.

The room temperature <sup>1</sup>H NMR spectrum of **5** in toluene-*d*<sub>8</sub> or in CD<sub>2</sub>Cl<sub>2</sub> exhibited three peaks in the ratio 3:3:1 assigned to the trispyrazolylborate ligands, the broadness of the resonance being due to the 3-methyls, suggesting that the fluxional process responsible for the equivalence of all the pyrazolyl rings is slow on the NMR time scale. The protons of the pyridinolate ligand gave two doublets and two triplets in the aryl region. Cooling **5** resulted in progressive broadening and shifting of the resonances associated with the pyrazolylborates. The resonances due to the protons on the pyridine ring shifted substantially,

(12) Sheldrick; G. M. *SHELXS-93: Program for Crystal Structure Refinement*; University of Göttingen:Göttingen, Germany, 1993.

(13) C<sub>35</sub>H<sub>48</sub>N<sub>13</sub>B<sub>2</sub>SeSm, fw = 901.89, monoclinic, space group *C*<sub>2</sub>/*m*, *a* = 17.593(2) Å, *b* = 11.977(3) Å, *c* = 20.040(3) Å, β = 91.94(1)°, *V* = 4220 Å<sup>3</sup>, *Z* = 4, ρ<sub>calc</sub> = 1.419 g cm<sup>-3</sup>. A total of 3900 unique reflections were used in the structure solution and refinement of 356 parameters. Final refinement converged at R1 = 0.083 and wR2 = 0.216 for 2912 reflections with  $I > 2\sigma(I)$ .

(14) (a) Berg, D. J.; Andersen, R. A.; Zalkin, A. *Organometallics* **1988**, *7*, 1858–1863. (b) Recknagel, A.; Noltemeyer, M.; Stalke, D.; Pieper, U.; Schmidt, H.-G.; Edelmann, F. T. *J. Organomet. Chem.* **1991**, *411*, 347–356. (c) Edelmann, F. T.; Rieckhoff, M.; Haiduc, I.; Silaghi-Dumitrescu, I. *J. Organomet. Chem.* **1993**, *447*, 203–208.

(15) (a) Khasnis D. V. V.; Buretea, M.; Emge, T. J.; Brennan, J. G. *J. Chem. Soc., Dalton Trans.* **1995**, 45–48. (b) Cheng, Y. F.; Emge, T. J.; Brennan, J. G. *Inorg. Chem.* **1994**, *33*, 3711–3714. (c) Kienitz, C. O.; Thöne, C.; Jones, P. G. *Inorg. Chem.* **1996**, *35*, 3990–3997.

(16) (a) Akita, M.; Otha, K.; Takahashi, Y.; Hikichi, S.; Moro-oka, Y. *Organometallics* **1997**, *16*, 4121–4128. (b) Lopes, I.; Lin, G. Y.; Domingos, A.; Marques, N.; Takats, J. *J. Am. Chem. Soc.* **1999**, *121*, 8110–8111.

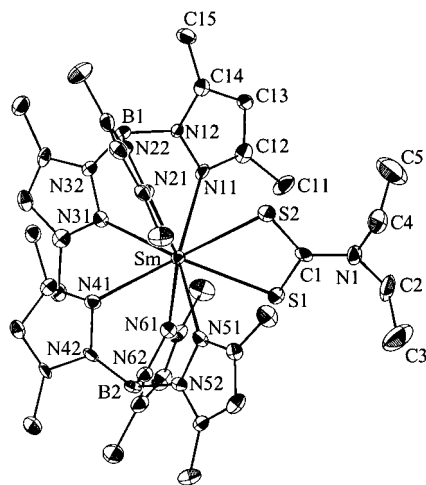


**Figure 1.** ORTEP diagram of  $[\text{Sm}(\text{Tp}^{\text{Me}_2})_2(\text{S}_2\text{CNET}_2)]$  (**1**), using 50% probability ellipsoids.

**Table 2.** Selected Bond Lengths [Å] and Angles (deg) for  $[\text{Sm}(\text{Tp}^{\text{Me}_2})_2(\text{XX}'\text{CNET}_2)]$  and  $[\text{Sm}(\text{Tp}^{\text{Me}_2})_2(\text{XC}_5\text{H}_4\text{X}')]$  ( $\text{X} = \text{X}' = \text{S}$  (**1**);  $\text{X}' = \text{N}$  and  $\text{X} = \text{S}$  (**3**),  $\text{Se}$  (**4**),  $\text{O}$  (**5**))

	<b>1</b>	<b>3</b> · $3\text{C}_6\text{H}_6$	<b>4</b>	<b>5</b>
Sm–X	2.891(2)	2.862(4)	3.00	2.355(3)
Sm–X'	2.873(2)	2.523(9)	2.53	2.480(4)
av(Sm–N)	2.63(10)	2.58(7)	2.55	2.60(7)
$\angle\text{X–Sm–X}'$	61.31(6)	57.5(2)	58	54.73(13)
$\angle\text{B}(1)\text{–Sm–B}(2)$	137.2	149.0	146	151.2
$\angle\text{Sm–X–C}(1)$	89.5(2)	82.9(5)	79	99.1(3)
$\angle\text{Sm–X}'\text{–C}(1)$	90.2(3)	104.6(8)	106	91.8(3)

because of the temperature dependence of the magnetic susceptibility, but suffered only minimal line broadening, and coupling remained resolved. By  $-80^\circ\text{C}$  the spectrum began to sharpen again and 12 resonances assigned to the methyl groups and 6 assigned to the methine protons of the pyrazolylborates were resolved, consistent with a  $C_1$ -symmetric coordination sphere.

To obtain information concerning the molecular structure of these compounds, which might account for the different barriers of the dynamic process occurring in solution, X-ray diffraction studies of the compounds were undertaken.

**Molecular Structures of  $[\text{Sm}(\text{Tp}^{\text{Me}_2})_2(\text{S}_2\text{CNET}_2)]$  (**1**) and  $[\text{Sm}(\text{Tp}^{\text{Me}_2})_2(\text{XC}_5\text{H}_4\text{N})]$  ( $\text{X} = \text{S}$  (**3**),  $\text{Se}$  (**4**),  $\text{O}$  (**5**)).** **Complex 1.** The molecular structure of **1** is shown in Figure 1, and selected bond lengths and angles are given in Table 2.

The structure consists of isolated molecules with no significant intermolecular contacts. The metal center is eight-coordinate, with the samarium atom bound in tridentate fashion by two pyrazolylborate ligands and in bidentate fashion by the dithiocarbamate ligand through both sulfur atoms. Polytopal analysis suggests that the metal coordination geometry is best described as being dodecahedral (DD).<sup>17</sup> Thus, the sulfur atoms lie on either side of the “pseudo- $S_4$ ” axis of the polyhedron, and the intersecting trapezoids (defined by the atoms N21, S2, S1, N61 and N11, N31, N41, N51, respectively) make a dihedral angle of  $78^\circ$  rather than the ideal  $90^\circ$ . While the trapezoid containing the sulfur atoms is almost planar, the second is somewhat distorted, as defined by the normalized  $\phi$  angles of  $0.3^\circ$  and  $10.9^\circ$ , respectively. Thus, the structure is rather similar to that observed previously for  $[\text{La}(\text{Tp}^{\text{Me}_2})_2(\text{NO}_3)]$  in which the nitrate group tightens the base of the dodecahedron and lowers the symmetry toward  $C_2$ .<sup>6</sup>

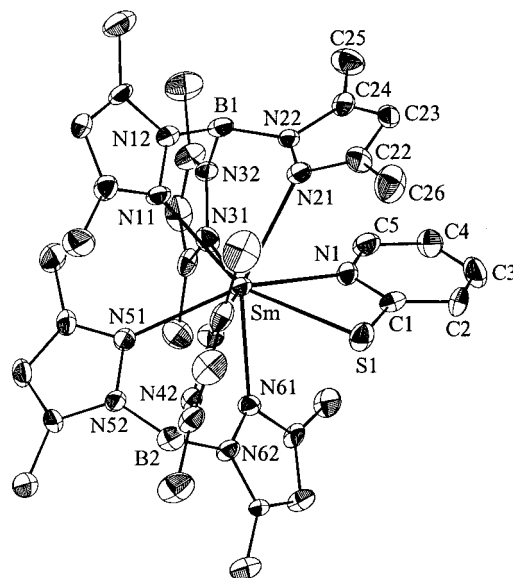


**Figure 2.** ORTEP diagram of  $[\text{Sm}(\text{Tp}^{\text{Me}_2})_2(\text{SC}_5\text{H}_4\text{N})]$  (**3**), using 30% probability ellipsoids.

The two pyrazolylborate groups are mutually staggered and bent back with a B–Sm–B angle of  $137.2^\circ$  comparable to that observed in  $[\text{Nd}(\text{Tp}^{\text{Me}_2})_2(\text{MeCN})_2](\text{O}_3\text{SCF}_3)$  ( $137^\circ$ ).<sup>6</sup> This bend angle is considerably smaller than in the comparable eight-coordinate complexes  $[\text{Sm}(\text{Tp}^{\text{Me}_2})_2(\text{O}_2)]$  ( $144.1^\circ$ ),<sup>5b</sup>  $[\text{Sm}(\text{Tp}^{\text{Me}_2})_2(\text{PhNNPh})]$  ( $152.6^\circ$ ),<sup>5a</sup>  $[\text{Sm}(\text{Tp}^{\text{Me}_2,4\text{-Et}})_2(\text{NO}_2)]$  ( $159.0^\circ$ ),<sup>18</sup>  $[\text{La}(\text{Tp}^{\text{Me}_2})_2(\text{NO}_3)]$  ( $143.6^\circ$ ),<sup>6</sup> and  $[\text{La}(\text{Tp}^{\text{Me}_2})_2(\text{MeCN})(\text{O}_3\text{SCF}_3)]$  ( $142.7^\circ$ )<sup>6</sup> and may be a reflection of the greater steric demand of the second-row donor atoms of the dithiocarbamate. This is probably also responsible for the longer average Sm–Npz distance in **1** (2.626(6) Å) (range 2.503(5)–2.728(5) Å) than in  $[\text{Sm}(\text{Tp}^{\text{Me}_2})_2(\text{O}_2)]$  (2.58 Å),<sup>5b</sup>  $[\text{Sm}(\text{Tp}^{\text{Me}_2})_2(\text{PhNNPh})]$  (2.59 Å),<sup>5a</sup> and  $[\text{Sm}(\text{Tp}^{\text{Me}_2,4\text{-Et}})_2(\text{NO}_2)]$  (2.559(4) Å).<sup>18</sup> The greater steric demand of  $\text{Tp}^{\text{Me}_2}$  relative to other ancillary ligands is evidenced in the smaller dithiocarbamate bite angle ( $\angle\text{S–Sm–S} = 61.31(6)^\circ$ ) and longer Sm–S bond lengths (2.891(2) and 2.873(2) Å) observed for **1**, against corresponding angles of  $64.1^\circ$  in  $[\text{Sm}(\text{Cp}^*)_2(\text{S}_2\text{CNMe}_2)]$ ,<sup>14b</sup>  $67.1(3)^\circ$  in  $[\text{Yb}(\text{Cp}^*)_2(\text{S}_2\text{CNET}_2)]$ ,<sup>19</sup> and  $65.6(1)^\circ$  in  $[\{\text{PhC}(\text{NTMS})_2\}_2\text{Yb}(\text{S}_2\text{CNMe}_2)]$ <sup>20</sup> and Sm–S distance for  $[\text{Sm}(\text{Cp}^*)_2(\text{S}_2\text{CNMe}_2)]$  of 2.808(2) Å.<sup>14b</sup> Pyrazolyl rings 1 (N11N12) and 5 (N51N52) are considerably twisted about their B–N bond, with B–N–N–Sm torsion angles of  $32.1^\circ$  and  $23.9^\circ$ , respectively.

**Complexes 3 and 4.** X-ray quality pale-yellow crystals of **3** were grown by slow diffusion of *n*-hexane into a benzene solution. The crystals also contained three benzene molecules per formula unit. Yellow crystals of **4** were grown from a toluene/hexane mixture and were not solvated. The molecular structure of **3** is shown in Figure 2 (**4** is not illustrated, but analogous atomic numbering schemes are used for **3** and **4**).

The structure consists of discrete monomeric molecular units in which the metal center is eight-coordinate with the samarium atoms bound in tridentate fashion by two pyrazolylborate ligands and in bidentate fashion by the chalcogenolate ligand. The coordination geometry around the Sm atom may again be described as being DD, the trapezoids being defined by the

(17) Drew, M. G. B. *Coord. Chem. Rev.* **1977**, *24*, 179–275.

(18) Maunder, G. H.; Sella, A. Unpublished results.

(19) Tilley, T. D.; Andersen, R. A.; Zalkin, A.; Templeton, D. H. *Inorg. Chem.* **1982**, *21*, 2644–2647.

(20) Wedler, M.; Noltemeyer, M.; Pieper, U.; Schmidt, H.-G.; Stalke, D.; Edelmann, F. T. *Angew. Chem., Int. Ed. Engl.* **1990**, *29*, 894–896.

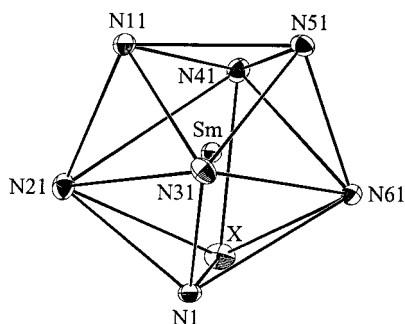


**Figure 3.** View of the dodecahedral coordination polyhedron of **3** and **4**.

atoms N41, X (X = S, Se), N1, N31 and N21, N11, N51, N61 for **3** and **4**, respectively, as shown in Figure 3.

Distortions from the DD geometries are defined by the dihedral angle of the intersecting trapezoids ( $83.0^\circ$  and  $82^\circ$ , respectively). The trapezoids containing the bidentate ligands are somewhat distorted, with normalized  $\varphi$  angles of  $19.6^\circ$  and  $4.3^\circ$  for **3** and **4**, respectively, and the second ones are almost planar (normalized  $\varphi$  angles of  $0.8^\circ$  and  $3.1^\circ$  for **3** and **4**, respectively). In **3** and **4**, there is greater distortion of the DD geometry along the pathway toward BCTP than was observed in the eight-coordinate complexes  $[\text{La}(\text{Tp}^{\text{Me}_2})_2(\text{MeCN})(\text{O}_3\text{SCF}_3)]$ ,  $[\text{La}(\text{Tp}^{\text{Me}_2})_2(\text{NO}_3)]$ , and  $[\text{Nd}(\text{Tp}^{\text{Me}_2})_2(\text{MeCN})_2][(\text{O}_3\text{SCF}_3)]$ .<sup>6</sup> This arrangement of the pyrazolyl groups and the bidentate ligand around the metal center results in an effective  $C_1$  symmetry consistent with the NMR evidence.

Comparative bond distances and angles are shown in Table 2. The two pyrazolylborate groups are mutually staggered and bent back with B–Sm–B angles of  $149.0^\circ$  and  $146^\circ$  for **3** and **4**, respectively. These bend angles are in the range found in the comparable eight-coordinate complexes  $[\text{Sm}(\text{Tp}^{\text{Me}_2})_2(\text{O}_2)]$  ( $144.1^\circ$ ),<sup>5b</sup>  $[\text{Sm}(\text{Tp}^{\text{Me}_2})_2(\text{PhNNPh})]$  ( $152.6^\circ$ ),<sup>5a</sup>  $[\text{Sm}(\text{Tp}^{\text{Me}_2,4\text{-Et}})_2(\text{NO}_2)]$  ( $159.0^\circ$ ),<sup>18</sup> and  $[\text{La}(\text{Tp}^{\text{Me}_2})_2(\text{MeCN})(\text{O}_3\text{SCF}_3)]$  ( $142.7^\circ$ ).<sup>6</sup> The average Sm–Npz bond lengths of  $2.58 \text{ \AA}$  (range  $2.477(10)$ – $2.676(11) \text{ \AA}$ ) in **3** and  $2.55 \text{ \AA}$  (range  $2.48$ – $2.68 \text{ \AA}$ ) in **4** are similar to those reported for the eight-coordinate  $[\text{Sm}(\text{Tp}^{\text{Me}_2})_2(\text{O}_2)]$ <sup>5b</sup> ( $2.58 \text{ \AA}$ ) and  $[\text{Sm}(\text{Tp}^{\text{Me}_2})_2(\text{PhNNPh})]$ <sup>5a</sup> ( $2.59 \text{ \AA}$ ) and shorter than the corresponding distance in **1** ( $2.63(10) \text{ \AA}$ ). The Sm–S and the Sm–N(1) bond distances in **3** ( $2.862(4)$  and  $2.523(9) \text{ \AA}$ , respectively) are slightly shorter than the corresponding values found in  $[\text{Sm}(\text{SC}_5\text{H}_4\text{N})_2(\text{HMPA})_3]\text{I}$  (av  $2.870(3)$  and  $2.542(7) \text{ \AA}$ , respectively)<sup>21</sup> and in  $[(\eta^8\text{-C}_8\text{H}_8)\text{Sm}(\text{SC}_5\text{H}_4\text{N})_2(\text{HMPA})_3]$  ( $2.932(7)$  and  $2.566(7) \text{ \AA}$ )<sup>22</sup> and are consistent with those in  $[(\text{py})_3\text{Yb}(\text{SC}_5\text{H}_4\text{N})_2]$  ( $2.889(2)$  and  $2.542(5) \text{ \AA}$ )<sup>23</sup> after adjustment for the difference in coordination number and ionic radii<sup>24</sup> and with those in  $[\text{PEt}_4][(\text{Eu}(\text{SC}_5\text{H}_4\text{N})_4)]$  ( $2.87(2)$  and  $2.52(1) \text{ \AA}$ ),<sup>25</sup> taking into account the difference of  $0.013 \text{ \AA}$  between the ionic radii of Sm(III) and Eu(III).<sup>24</sup> The Sm–Se bond distance of  $3.00 \text{ \AA}$  in **4** is longer than the corresponding distance in the seven-coordinate  $[\text{Sm}(\text{Tp}^{\text{Me}_2})_2(\text{SePh})]$  ( $2.9390(3) \text{ \AA}$ )<sup>26</sup> but is in line with the value of  $2.862(4) \text{ \AA}$  in **3** after correction for the difference in atomic radius between S and Se. Interestingly the Sm–Se distance in **4** is

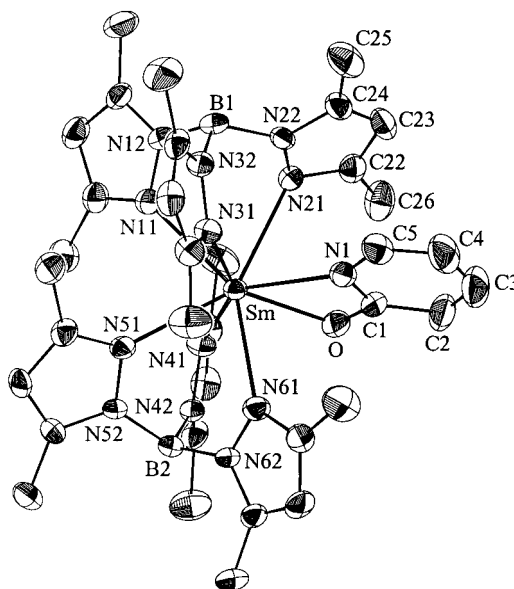


**Figure 4.** ORTEP diagram of  $[\text{Sm}(\text{Tp}^{\text{Me}_2})_2(\text{OC}_5\text{H}_4\text{N})]$  (**5**), using 40% probability ellipsoids.

longer than in the highly distorted pseudo-eight-coordinate molecules  $[\text{Sm}(\text{Tp}^{\text{Me}_2})_2(\text{SeC}_6\text{H}_4\text{R})]$  (R = H  $2.9621(3) \text{ \AA}$ ; R = Me  $2.9457(3) \text{ \AA}$ ).<sup>26</sup> The different Sm–N(1) and Sm–S(Se) distances result in markedly different Sm–S(Se)–C(1) and Sm–N(1)–C(1) bond angles ( $82.9(5)^\circ$  and  $104.6(8)^\circ$ , and  $79^\circ$  and  $106^\circ$  for **3** and **4**, respectively), leading to the bending of the chalcogenolate ligand toward pyrazolyl N21. As a result, the pyrazolyl rings closer to the bidentate ligands (N21N22 and N61N62) are considerably twisted about their B–N bonds, with B–N–N–Sm torsion angles of  $56.1/35.7^\circ$  and  $39/25^\circ$ , respectively.

**Complex 5.** Complex **5** crystallized from a toluene/hexane mixture as transparent plates. The molecular structure is shown in Figure 4. The structure is similar to those reported for **3** and **4**, with two tridentate pyrazolylborate ligands and the pyridinolate in the first coordination sphere of the samarium. The arrangement of the donor atoms lends effective  $C_1$  symmetry to the binding site. The coordination geometry is once more best regarded as being DD with a dihedral angle of the intersecting trapezoids of  $81.5^\circ$  and normalized  $\varphi$  angles of  $1.3^\circ$  and  $0.5^\circ$ . The two  $\text{Tp}^{\text{Me}_2}$  ligands are mutually staggered and bent back from each other at an angle of  $151.2^\circ$  (Table 2). This value is greater than those in **1**, **3**, and **4** and reflects the smaller size of the pyridinolate ligand. The Sm–O bond distance ( $2.355(3) \text{ \AA}$ ) is comparable with the average bond distance of  $2.325(3) \text{ \AA}$  in the eight-coordinate  $[\text{Sm}(\text{Tp}^{\text{Me}_2})_2(\text{O}_2)]$ <sup>5b</sup> but is much longer than those reported for the seven-coordinate  $[\text{Sm}(\text{Tp}^{\text{Me}_2})_2(\text{OPh-4-Bu}^t)]$  ( $2.159(2) \text{ \AA}$ ),<sup>26</sup>  $[\text{Sm}(\text{Tp}^{\text{Me}_2})_2(\text{OPh-2,4,6-Bu}^t)]$  ( $2.188(2) \text{ \AA}$ ),<sup>27</sup>  $[\text{Sm}(\text{Tp}^{\text{Me}_2})_2(\text{OCPh}_2)]$  ( $2.201(3) \text{ \AA}$ ),<sup>5d</sup> and  $[\text{Sm}(\text{Tp}^{\text{Me}_2})_2(\text{OC}_6\text{H}_2(\text{Bu}^t)_2\text{O})]$  ( $2.213 \text{ \AA}$ ).<sup>5c</sup> The unusually long Sm–O bond length in **5** therefore reflects the strain associated with the four-membered chelate ring. Owing to the small bite of the pyridinolate ligand, the angles in the chelate ring are significantly reduced from their normal values, with Sm–O–C(1) and O–Sm–N(1) bond angles of  $99.1(3)^\circ$  and  $54.7(1)^\circ$ , respectively. The proximity of the bidentate ligand to the Sm center leads to severe twisting of the pyrazolyl rings N2 (N21N22) and N4 (N41N42), with B–N–N–Sm torsion angles of  $58/28^\circ$ .

**<sup>1</sup>H NMR Studies. Fluxionality of 1–5.** As noted previously, compounds **1–5** are all fluxional, with **5** being in rapid exchange

(21) Mashima, K.; Shibahara, T.; Nakayama, Y.; Nakamura, A. *J. Organomet. Chem.* **1995**, *501*, 263–269.

(22) Mashima, K.; Shibahara, T.; Nakayama, Y.; Nakamura, A. *J. Organomet. Chem.* **1998**, *559*, 197–201.

(23) Berardini, M.; Lee, J.; Freedman, D.; Lee, J. L.; Emge, T. J.; Brennan, J. G. *Inorg. Chem.* **1997**, *36*, 5772–5776.

(24) Shannon, R. D. *Acta Crystallogr.* **1976**, *A32*, 751–767.

(25) Berardini, M.; Brennan, J. G. *Inorg. Chem.* **1995**, *34*, 6179–6185.

(26) Hillier, A. C.; Liu, S. Y.; Sella, A.; Elsegood, M. R. *J. Inorg. Chem.* **2000**, *39*, 2635–2644.

(27) Lopes, I.; Domingos, A.; Marques, N. Unpublished results.

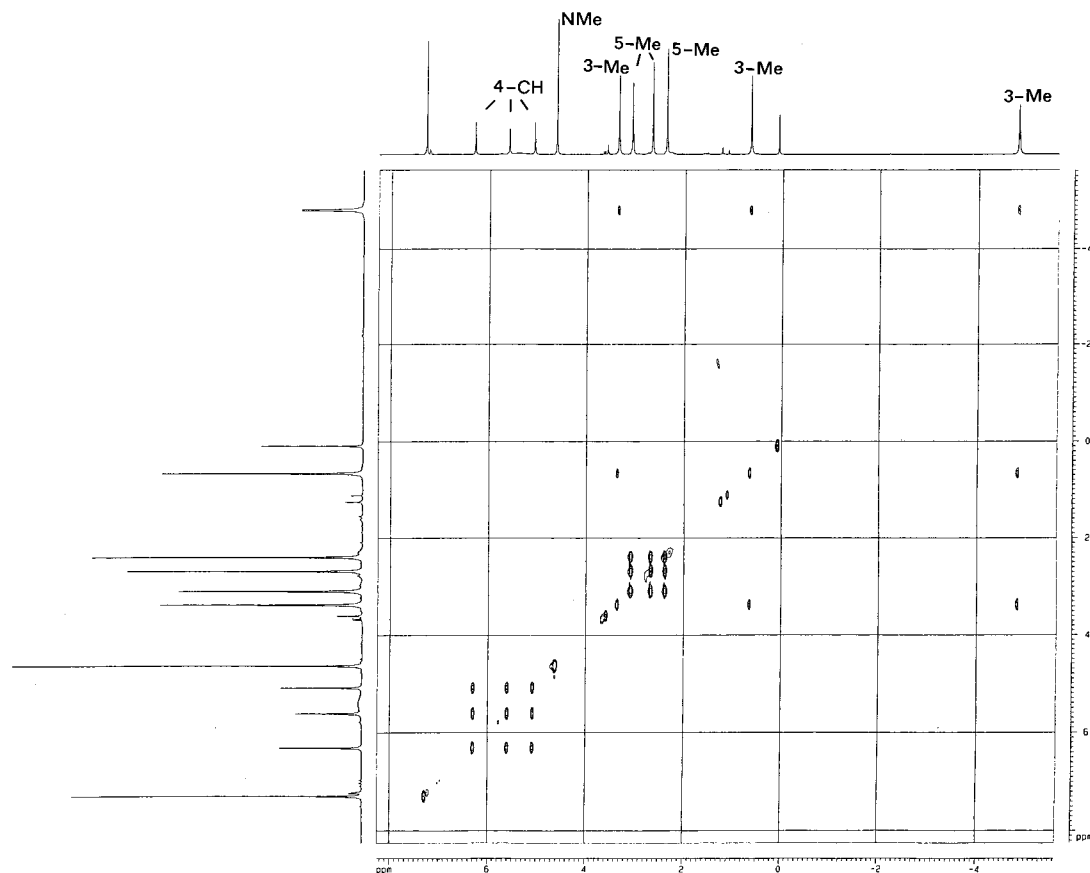


Figure 5. A 500 MHz  $^1\text{H}$ – $^1\text{H}$  EXSY NMR spectrum of  $[\text{Sm}(\text{Tp}^{\text{Me}_2})_2(\text{S}_2\text{CNMe}_2)]$  (**2**), recorded in  $\text{CDCl}_3$  at  $-20^\circ\text{C}$ .

at room temperature. Because of their overall structural similarity, it is reasonable to suppose that the coordination spheres of these five complexes rearrange by similar processes, although the stereochemical lability of **5** may point toward a different mechanism (vide infra).

The 2D EXSY experiment provides a convenient method for obtaining qualitative maps of the fluxionality of complex molecular systems.<sup>28</sup> To probe the exchange pathways of these complexes,  $^1\text{H}$  phase-sensitive EXSY experiments were performed on **1**–**4**. The EXSY spectrum of **2** (Figure 5) shows a pair of cross-peaks for each resonance, indicating that the pyrazolyl rings are in slow exchange with each other at  $-20^\circ\text{C}$ . No antiphase cross-peaks, indicative of the nuclear Overhauser effect (NOE), were observed in any of the spectra.

These cross-peaks also allow definitive assignment of the methyl groups to the 3 and 5 positions of the pyrazolyl groups; in common with other  $\text{Sm}(\text{Tp}^{\text{Me}_2})_2$  systems, the 3-methyls, being closer to the samarium center, show a much greater variation in chemical shift than those in the 5-position. Thus, at first sight, this experiment implies that the  $\text{Tp}^{\text{Me}_2}$  groups simply rotate about the  $\text{Sm}$ – $\text{B}$  axis. By contrast, the corresponding EXSY spectra of **3** and **4** are rather more informative and give evidence for two distinct dynamic regimes. At room temperature the EXSY spectra of these compounds (the spectrum of **3** is shown in Figure 6) show cross-peaks connecting four of the six pairs of methyl groups and two of the three pairs of methine peaks.

Thus, *only four* pyrazolyl groups undergo measurable exchange at this temperature. This mechanism will be denoted the low-temperature process (LTP). When the samples are warmed to  $40^\circ\text{C}$ , the exchange of all six pyrazolyl rings is observed (Figure 7). This process is denoted as the high-

temperature process (HTP). We note that by this temperature the LTP is sufficiently rapid to broaden 12 of the singlets relative to the remaining 6.

Because the various eight-coordination polyhedra are readily interconverted by relatively small displacements of the ligand donor atoms, polytopal rearrangement mechanisms have often been invoked to explain the fluxionality found in solution of eight-coordinate complexes.<sup>29</sup> For example, interchange between two SAP forms via a BCTP intermediate has been the mechanism proposed by Takats to explain the fluxionality of the complexes  $[\text{Ln}(\text{HBp}_3)_2(\text{dik})]^{30}$  ( $\text{dik} = \beta$ -diketonate) and by Santos to interpret the solution behavior of  $\text{U}(\text{HBp}_3)_2\text{XY}$  complexes.<sup>31</sup> Interconversion of the three coordination geometries has been invoked by Marçalo to explain the magnetic equivalence of the pyrazolyl rings in  $[\text{Th}(\text{HBp}_3)_2\text{XY}]$  complexes.<sup>32</sup> Polytopal rearrangements between two dodecahedral stereoisomers via a SAP intermediate have been considered as the preferred path for rearrangements in tetrakis( $\beta$ -diketonates) of  $\text{Zr}(\text{IV})$ ,  $\text{Hf}(\text{IV})$ , and  $\text{Th}(\text{IV})^{33}$  and in tetrakis( $N,N$ -dialkyl-dithiocarbamates) of  $\text{Ti}(\text{IV})$  and  $\text{Zr}(\text{IV})$ .<sup>34</sup> Thus, the interconversion among the SAP, DD, and BCTP geometries provides a way to rationalize the movements of the donor atoms in the

(29) (a) Kepert, D. L. *Prog. Inorg. Chem.* **1977**, *24*, 179–249. (b) Porai-Koshits, M. A.; Aslanov, L. A. *J. Struct. Chem.* **1972**, *13*, 244–253. (c) Muetterties, E. L.; Guggenberger, L. J. *J. Am. Chem. Soc.* **1974**, *96*, 1748–1756.

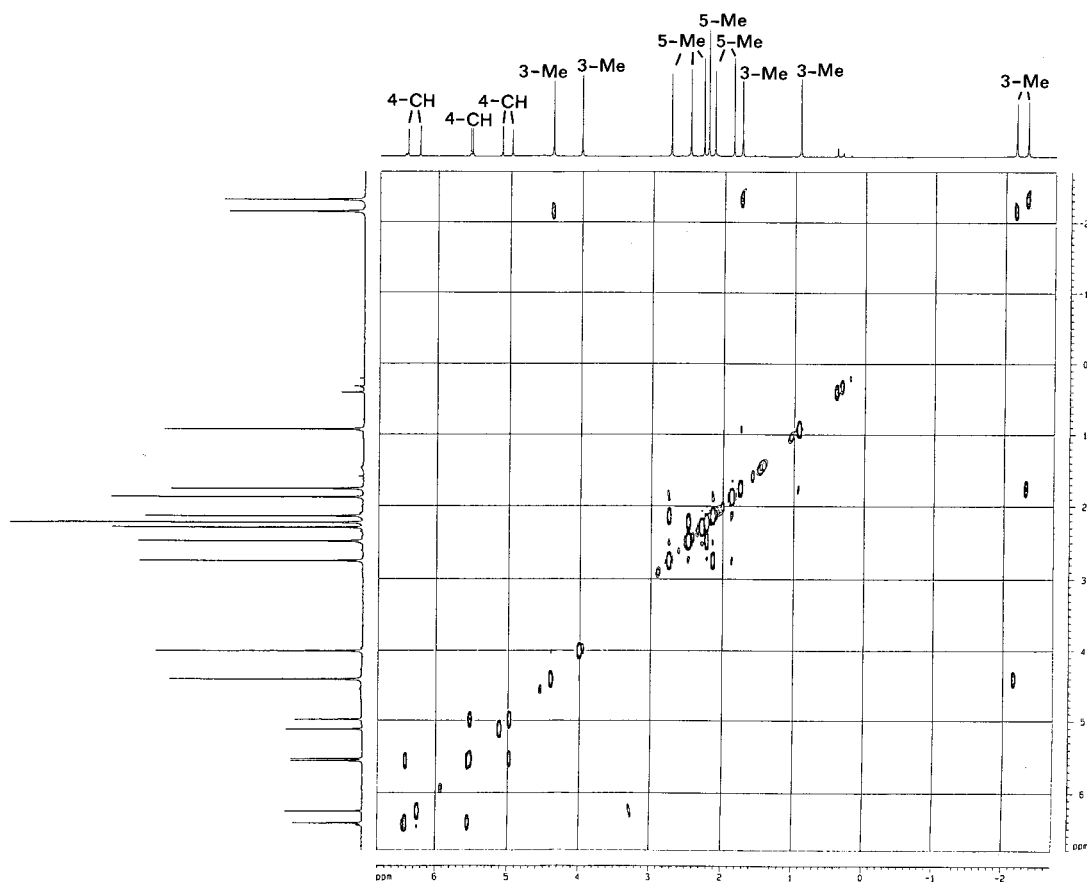
(30) Moffat, W. D.; Stainer, M. V. R.; Takats, J. *Inorg. Chim. Acta* **1987**, *139*, 75–78.

(31) Santos, I. Ph.D. Thesis, Instituto Superior Técnico, Lisboa, Portugal, 1990.

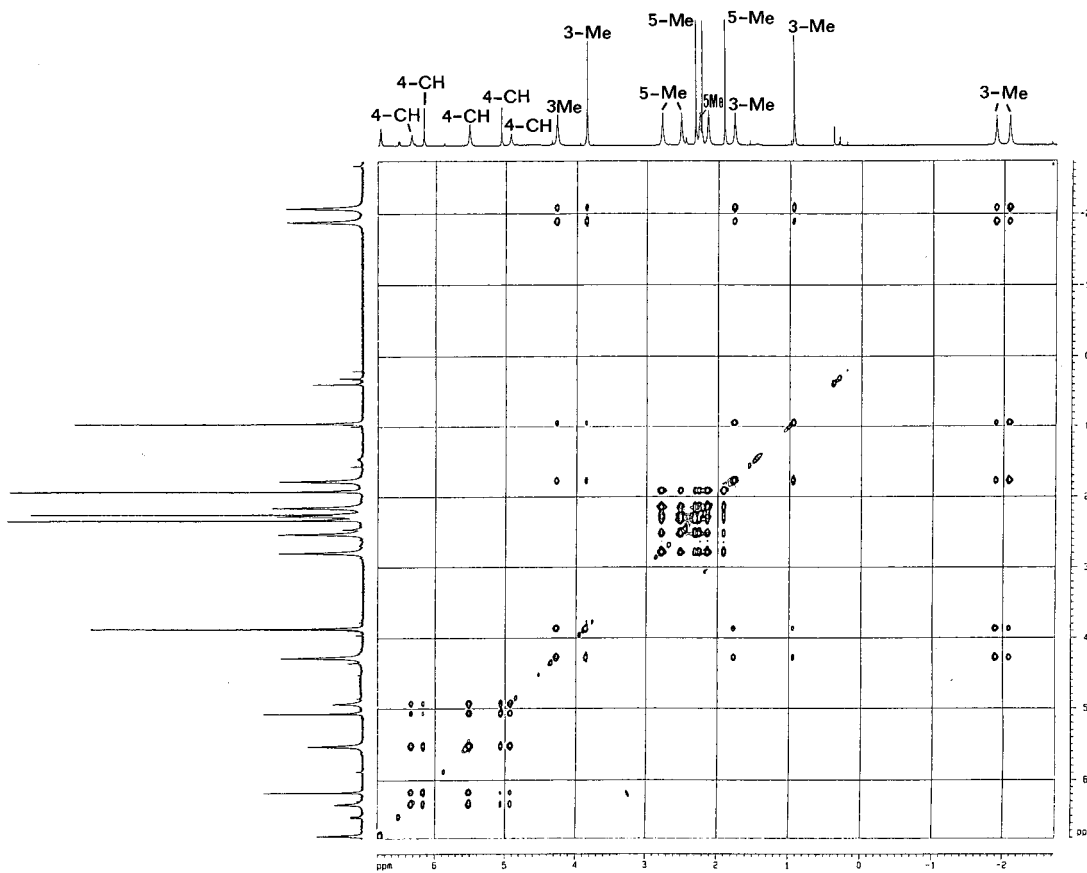
(32) Marçalo, I. Ph.D. Thesis, Instituto Superior Técnico, Lisboa, Portugal, 1990.

(33) Fay, R. C.; Howie, J. K. *J. Am. Chem. Soc.* **1979**, *105*, 1115–1122.

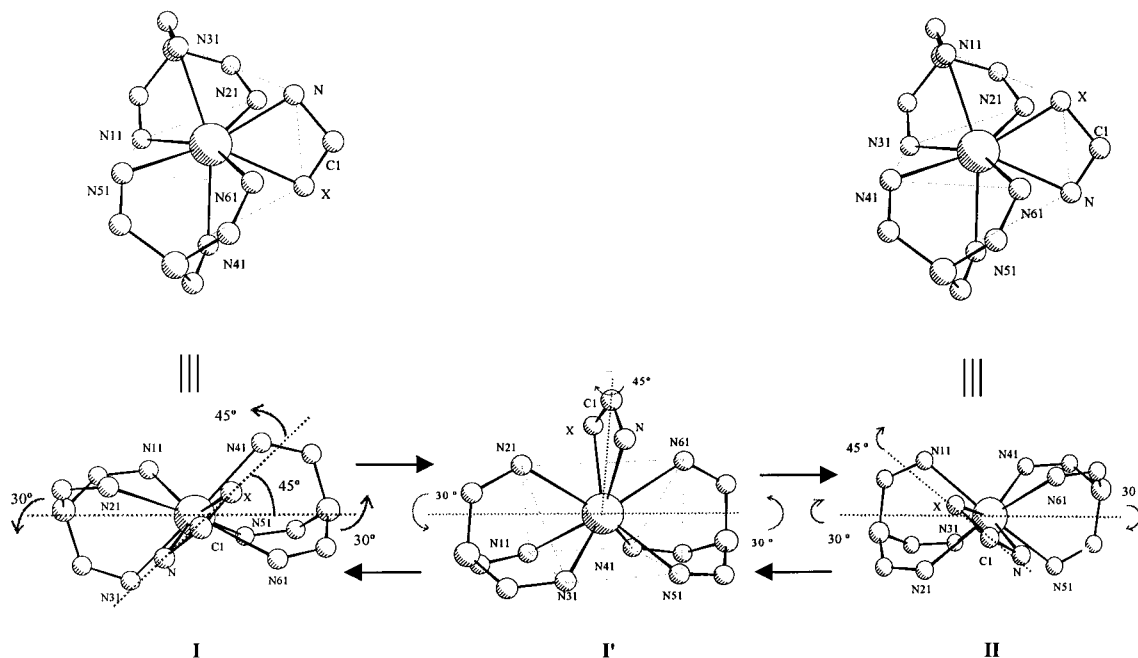
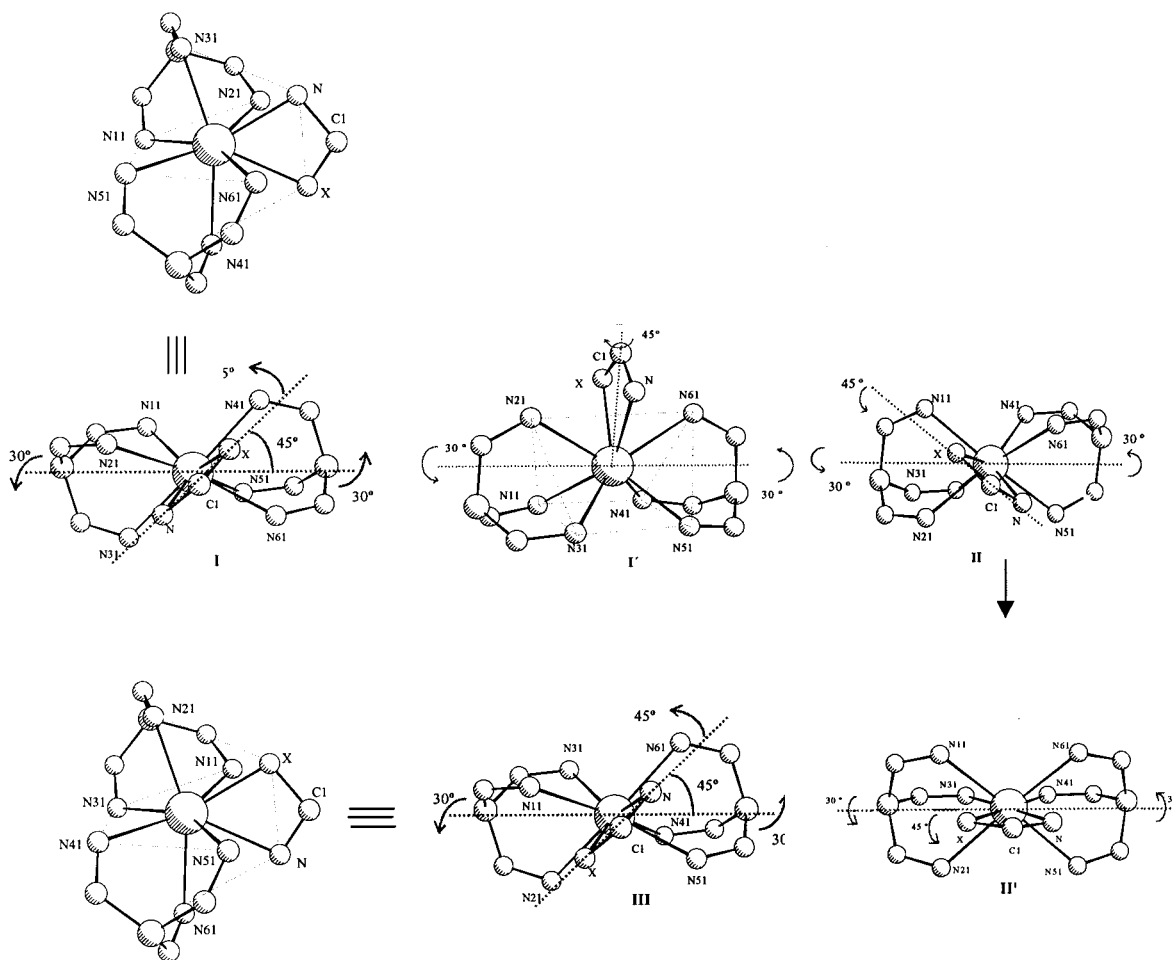
(34) Hawthorne, S. L.; Bruder, A. H.; Fay, R. C. *Inorg. Chem.* **1983**, *22*, 3368–3375.



**Figure 6.** A 500 MHz  $^1\text{H}$ - $^1\text{H}$  EXSY NMR spectrum of  $[\text{Sm}(\text{Tp}^{\text{Me}_2})_2(\text{SC}_5\text{H}_4\text{N})]$  (**3**), recorded in toluene- $d_8$  at 20 °C.



**Figure 7.** A 500 MHz  $^1\text{H}$ - $^1\text{H}$  EXSY NMR spectrum of  $\text{Sm}(\text{Tp}^{\text{Me}_2})_2(\text{SC}_5\text{H}_4\text{N})$  (**3**), recorded in toluene- $d_8$  at 40 °C. Note excess broadening of the peaks involved in LTP.

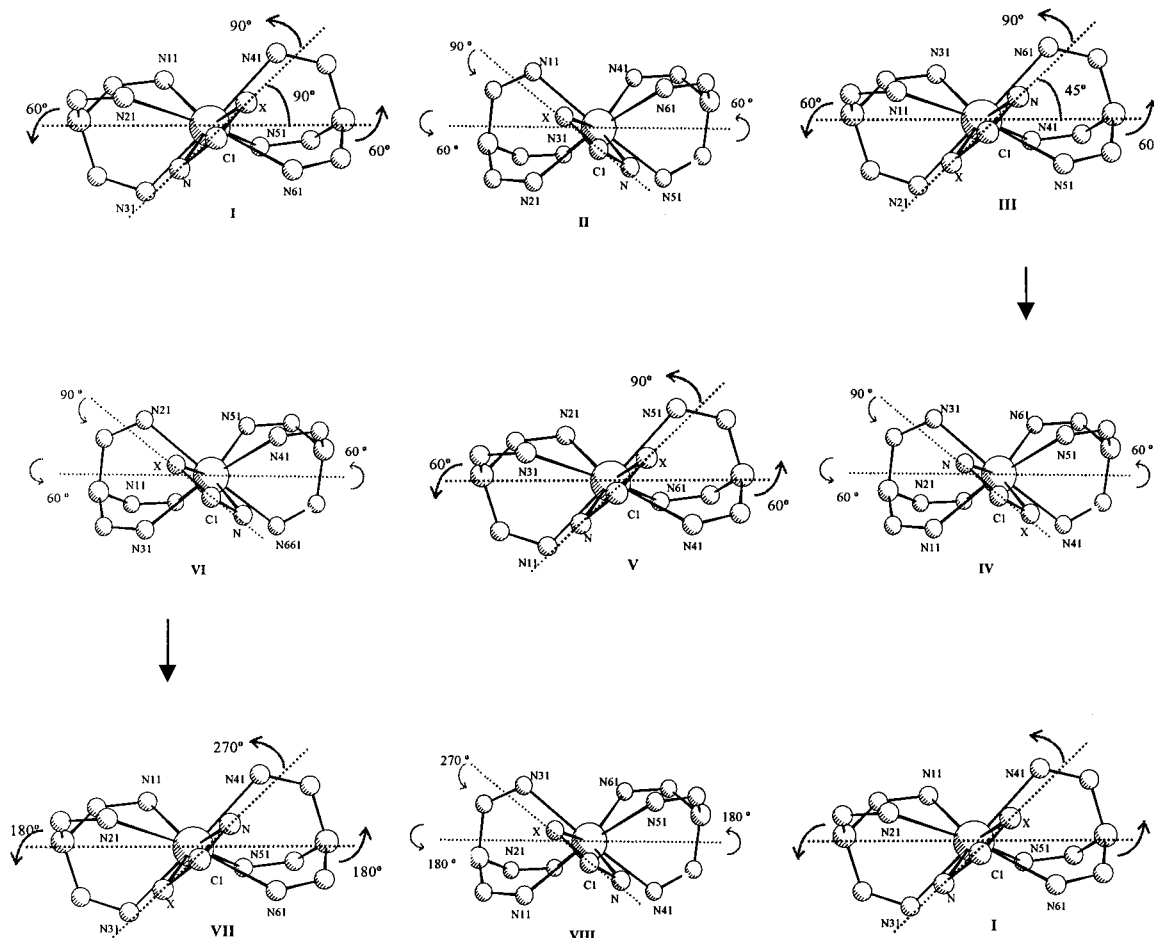
**Scheme 1.** Low-Temperature (LTP) Exchange Process Responsible for Pairwise Exchange of Pyrazolyl Groups in **3** and **4****Scheme 2.** High-Temperature (HTP) Exchange Process (Detailed View of Initial Bidentate Ligand Rotation) Responsible for Complete Exchange of Pyrazolyl Groups

coordination spheres of the central ions. Unfortunately this is difficult to visualize easily in the case of these systems. A conceptually simpler but entirely equivalent way of describing the rearrangements is to consider that the movements of the

donor atoms in the coordination sphere of the metal can occur by a concerted, effectively gear-locked rotation of the ligands.

The mechanisms we propose to account for the observed fluxionality of **3** and **4** are shown in Schemes 1 (LTP) and 2



**Scheme 3.** High-Temperature (HTP) Exchange Process (Full View) Responsible for Complete Exchange of Pyrazolyl Groups

and 3 (HTP). The LTP may be envisaged as occurring as follows. Twisting the two Tp ligands in opposite directions by  $30^\circ$  around their respective Sm–B vectors accompanied by twisting of the plane of the bidentate ligand by  $45^\circ$  (i.e., rotation of the chelate by  $45^\circ$  around the samarium–ligand axis running between the two donor atoms) results in an intermediate BCTP structure (**I**). Note that in this intermediate (**I**) the bidentate ligand lies effectively perpendicular to the plane defined by the samarium and boron atoms. Second, throughout this motion the plane of the bidentate ligand is maintained perpendicular to that defined by Sm, N21, and N61. Comparison of structures **I** and **II** shows that this motion maintains pyrazolyl rings N2 and N6 in the same coordination environment while interchanging pyrazolyl groups N1 with N3 and N5 with N4 in pairwise fashion.

The HTP may now be considered to be simply an extension of this libration in which both ligands rotate beyond the  $30^\circ$  and  $45^\circ$  required for the LTP. Steric interactions between the bidentate ligands and the N2 and N6 rings result in a significant barrier to further rotation. As shown by our NMR experiments, this motion only becomes significant above  $40^\circ\text{C}$ . Concerted rotation of the three ligands results in the intermediate structure (**II**), before returning to another stable DD configuration (**III**) (Scheme 2).

Note that in structure **III** the bidentate ligand now lies in the plane of Sm, N21, and N61. Comparison of **I** with **III** shows that exchange of the three pairs of pyrazolyl rings between different coordination sites of the DD configuration has occurred. Within a molecule of  $C_1$  symmetry, full exchange of

the pyrazolyl rings can only be achieved by allowing the tridentate ligands to rotate by  $2 \times 360^\circ$  and the bidentate ligand by  $3 \times 360^\circ$ , when the ground state configuration is again achieved. This is illustrated in Scheme 3 from which the intermediates have been omitted and only rotations of  $60^\circ$  (from **I** to **VI**) and  $180^\circ$  (from **VII** to **IX**) are illustrated.

The scheme shows how these rotations average the chemical environment of each pyrazolyl ring, giving rise to magnetically equivalent protons.

In the case of **1** we have been unable to observe the pairwise exchanges analogous to the LTP observed for **3** and **4**. This may suggest that the longer Sm–S distances imply smaller steric interactions between the dithiocarbamate ligand and pyrazolyl rings N21 and N61 resulting in a lower barrier to the HTP process, compared with those of **3** and **4**. In addition, the structural data point toward an increase in steric crowding in the asymmetric systems as evidenced by the bending of the bidentate ligands toward pyrazolyl ring N21. In parallel work, we have observed that the rate of fluxionality in similar complexes  $[\text{Nd}(\text{Tp}^{\text{Me}_2})_2(\text{dik})]$  varies in the order  $\text{acac} > \text{dipivaloylmethane} > \text{dibenzoylmethane}$ , highlighting the importance of steric interactions.<sup>35</sup>

On this basis, therefore, we can account for the observed EXSY spectra of **1**, **3**, and **4**. Such mechanisms also account for the magnetic equivalence of all pyrazolyl rings for **5**, a faster rearrangement being expected for this compound because of the decreased steric demand of the  $\text{NC}_5\text{H}_4\text{O}$  ligand. However, the difference in rates is somewhat puzzling and may perhaps

(35) Goodchild, S.; Sella, A. Unpublished observations.

indicate that there is a different mechanism for this complex. A number of alternatives may be envisaged. Intermolecular mechanisms can be reasonably excluded on the basis of the following experiments: (a) the variable temperature  $^1\text{H}$  NMR spectra of **5** in  $\text{CD}_2\text{Cl}_2$  are independent of concentration ( $4.77 \times 10^{-2}$ ,  $1.59 \times 10^{-2}$  M); (b) in the NMR spectrum of a mixture of **5** and a stoichiometric amount of the analogous neodymium compound  $[\text{Nd}(\text{Tp}^{\text{Me}_2})_2(\text{OC}_3\text{H}_4\text{N})]$  (**6**), the chemical shifts, line widths, and the coupling patterns of the resonances due to the protons of the Opy ligands of **5** and **6** were identical to those observed for pure samples.

An alternative intramolecular mechanism can be proposed in which rupture of the Sm–pyridine bond in **5** occurs with formation of a seven-coordinate intermediate. Rapid rearrangement of the coordination sphere and subsequent ring closure then regenerate the initial chelate. Teuben and co-workers have suggested that  $[\text{Cp}^*\text{Y}(o\text{-C}_6\text{H}_4\text{CH}_2\text{NMe}_2)_2]$  rearranges by this type of mechanism.<sup>36</sup> The reduced coordination number in the intermediate would reduce the steric constraints on the ligands very significantly. Indeed, we note that our previous attempts to slow the fluxionality of the analogous seven-coordinate phenoxide  $[\text{Sm}(\text{Tp}^{\text{Me}_2})_2\text{OPh}]$  were not successful.<sup>26</sup> The difference in the donor properties of O and S (Se) may be responsible for the difference in the solution behavior, the Opy ligand being a better donor than the ligands containing S or Se atoms may weaken the Sm–pyridine bond, thus facilitating Sm–N bond breaking. An alternative view is that the electronegativity of the oxygen reduces the electron density on N, making the pyridine a less effective ligand in **5** than in **3** and **4**. Furthermore, the angles in the four-membered chelate ring are significantly reduced from their normal values as a result of the small bite of the  $\text{NC}_5\text{H}_4\text{O}$  ligand. The increased strain in the Opy system would therefore facilitate the bond-breaking process.

(36) Boojj, M.; Kiers, N. H.; Meetsma, A.; Teuben, J. H.; Smeets, W. J. J.; Spek, A. L. *Organometallics* **1989**, *8*, 2454–2461.

## Conclusions

In this work we have prepared a set of eight-coordinate samarium complexes by reductive cleavage of dichalogenides or by metathesis. These apparently simple complexes have been crystallized, and all show dodecahedral coordination geometries around the samarium center. The complexes are fluxional, and the  $\text{Tp}^{\text{Me}_2}$  ligands act as useful stereochemical probes of the system. The 2D NMR experiments suggest that the mechanism involves metal-centered rearrangements between different coordination geometries. The rate of the mechanism is controlled by steric interactions between the ligands, which are to some extent gear-locked at these crowded centers. Although related rearrangements have been reported before, our use of an unsymmetrical bidentate ligand results in much more detailed information about the dynamics. In particular we have been able to observe subtle differences in the barriers to the rotations of the various ligands, which point toward the potential for steric control in these systems.

**Acknowledgment.** Financial support from PRAXIS XXI (2/2.1/QUI/454/94) (N.M.) is gratefully acknowledged. I.L. thanks PRAXIS XXI for a Ph.D. grant. We are grateful to the EPSRC for a studentship for A.C.H. (GR/K11338) and to the Formosa Chemical Company for study leave for S.Y.L. We thank the EPSRC crystallography service for data collection (**1**). Dr. Abil Aliev is thanked for assistance in acquiring the NMR spectra, and Prof. J Takats and Dr. J. Marçalo are thanked for helpful discussions. We are also grateful to Prof. J. G. Brennan for drawing our attention to ref 15.

**Supporting Information Available:** X-ray crystallographic files, in CIF format, for the crystal structures of  $[\text{Sm}(\text{Tp}^{\text{Me}_2})_2(\text{S}_2\text{CNEt}_2)]$ ,  $[\text{Sm}(\text{Tp}^{\text{Me}_2})_2(\text{SC}_3\text{H}_4\text{N})] \cdot 3\text{C}_6\text{H}_6$ , and  $[\text{Sm}(\text{Tp}^{\text{Me}_2})_2(\text{OC}_3\text{H}_4\text{N})]$ .

IC001056X